SPACE- AND GROUND-BASED INVESTIGATIONS OF SOLAR WIND-MAGNETOSPHERE-IONOSPHERE COUPLING

S. E. Milan, J. A. Wild[1], A. Grocott, and N. C. Draper

Department of Physics and Astronomy,
University of Leicester,
Leicester LE1 7RH,
U.K.

[1]Now at: Department of Communication Systems, Lancaster University, Lancaster LA1 4WA, U.K.

Abstract.

This paper provides a brief review of the understanding of the coupled solar wind-magnetosphere-ionosphere system that can be attained from observations of the size of the ionospheric polar caps from space and the ground. These measurements allow the occurrence and rate of dayside and nightside reconnection to be deduced. The former can be correlated with upstream interplanetary magnetic field observations to give an estimate of the effective length of the dayside reconnection X-line. The latter allows a preliminary statistical study of flux closure during substorms and other, smaller nightside reconnection events.

1. Introduction

The form, dynamics and energy-throughput of the magnetosphere are determined by the rates of magnetic reconnection at the magnetopause and in the magnetotail. Together these control the proportion of terrestrial field lines that are interconnected with the solar wind, allowing ingress and egress of plasma across the magnetopause, and coupling solar wind momentum into the magnetosphere to drive magnetospheric and ionospheric convection. The fraction of the 8 GWb of flux associated with each hemisphere of the Earth that is at any instant interconnected to the interplanetary magnetic field varies between 2% and perhaps 15% on timescales as short as tens of minutes (Milan *et al.*, 2004). This proportion increases when the interplanetary magnetic field (IMF) is directed southwards and sub-solar reconnection at the magnetopause transforms closed field lines to an open topology (Dungey, 1961, 1963). The accumulation of flux causes the ionospheric polar cap to expand and the auroral

oval to move to lower latitudes, and is consequently sometimes referred to as the "substorm growth phase". Reconnection in the magnetotail, often associated with substorm break-up, closes open flux and causes the polar cap to contract; the appearance and development of the break-up aurora associated with the substorm has resulted in the name "substorm expansion phase". It now appears that there are also intervals of tail reconnection that are not associated with the classic signatures of substorms (e.g. break-up aurora, magnetogram bays), which often occur during periods of northward IMF (Grocott *et al.*, 2003, 2004; Milan *et al.*, 2005b). When the IMF is directed northwards dayside reconnection no longer occurs between closed terrestrial field lines and the IMF, but with lobe field lines – field lines that are already open (e.g. Russell, 1972; Cowley, 1981; Reiff and Burch, 1985; Cowley and Lockwood, 1992). In this situation the amount of open flux in the magnetosphere does not change but that which is present is "stirred".

The level of reconnection at the magnetopause or in the magnetotail cannot be determined from point observations in space, as reconnection X-lines are expected to be many Earth radii in extent. However, the ionospheric footprints of these X-lines, or merging gaps, can be mapped by ground-based radars or space-based auroral imagers, allowing their dynamics and extent to be determined. Ionospheric plasma flow across a merging gap allows the reconnection electric field to be measured, which if known along the whole length of the merging gap, gives the overall reconnection voltage (e.g. Baker *et al.*, 1997; Pinnock and Rodger, 2001; Grocott *et al.*, 2002; Milan *et al.*, 2003, Chisham *et al.*, 2004). Alternatively, if the boundary between open and closed field lines (the open/closed field line boundary or OCB) can be determined in the ionosphere, then the open flux content of the magnetosphere can be quantified, from which it is possible to deduce the reconnection rates (e.g. Taylor *et al.*, 1996; Mishin *et al.*, 1997; Milan *et al.*, 2003, 2004, 2005b; Milan, 2004b). It is the purpose of the present paper to review how such measurements are made and describe our current understanding of the dynamics of the system.

2. Measuring the open flux content of the magnetosphere

The open flux of the magnetotail lobes maps to the northern and southern ionospheric polar caps. The amount of open flux F_{PC} is found by integrating the radial

component of the magnetic field $\boldsymbol{B}$ (assumed dipolar) over either of the polar caps (F_{PC} is necessarily equal in each):

$$F_{PC} = \int_{PC} \boldsymbol{B} \cdot d\boldsymbol{s} \,. \tag{1}$$

This requires that the extent of the polar cap is known, or in other words that the latitude of the open/closed field line boundary (OCB) can be found at all local times. This is most readily identified by the particle populations residing on either side of the boundary, and the impact that these have on the ionosphere. On closed field lines, equatorward of the boundary, high energy (several—100s keV) are trapped as they mirror between the conjugate hemispheres. Once field lines are opened, however, particles are no longer trapped and are rapidly lost to the magnetotail. Solar wind plasma can gain entry to the magnetosphere on recently opened field lines, though these mirror only once before populating the mantle. Hence at low altitudes, high energy particles (esp. accelerated by the reconnection process) can be observed on open field lines downstream of the dayside merging gap, though these can be recognized and distinguished from trapped particles by their characteristic dispersed – and sometimes stepped – nature (e.g. Lockwood and Smith, 1992).

The OCB can be found, then, by determining the poleward edge of the trapped particle region. Several techniques can be used, but the most obvious is by direct measurement of the precipitating particle populations by polar-orbiting satellites (e.g. Sotirelis *et al.*, 1998). This technique has the disadvantage that such spacecraft can identify the boundary only along their orbit, that is at two points in each pass of the polar regions. Alternatively, global auroral imaging from space allows the aurora generated by the trapped particles to be identified over the whole of the polar region (e.g. Frank and Craven, 1988). Care must be taken with this technique as different cameras will have different detection thresholds and are sensitive to precipitation of particles in different energy regimes. Also, in summer, the dayside oval can be obscured by dayglow. Furthermore, the orbits of present imagers are such that continuous observation of the polar regions are only possible for periods of 8—12 hours. Other techniques for identifying the OCB include detection of the ionospheric electron density enhancement produced by precipitating trapped particles, for instance with an incoherent scatter radar (e.g. de la Beaujardiere *et al.*, 1991; Blanchard *et al.*, 2001), and identification of the spectral width boundary observed by coherent radars

(e.g. Chisham and Freeman, 2003). Ideally, a combination of some or all of these measurement techniques can be used to improve accuracy (Milan *et al.*, 2003). Recently, intercalibration of the different techniques has been undertaken (e.g. Wild *et al.*, 2004; Chisham *et al.*, 2005). It is difficult to assess the uncertainty in the measurement of F_{PC}, but assuming that the latitude of the OCB is over- or underestimated by 1° at all local times leads to an error margin of ±10% (Milan *et al.*, 2003).

Using these techniques several intervals have been analysed to determine the variation of F_{PC} with time. Three such intervals, 5 June 1998 (Milan *et al.*, 2003), 26 August 1998 (Milan *et al.*, 2004), and 19 January 2002 (Milan *et al.*, 2005b), are shown in Figure 1. F_{PC} is shown by the grey curves in panels a, f, and k, and can be seen to vary between approximately 0.2 and 1.0 GWb, that is between 2.5 and 12% of the flux associated with the Earth's magnetic field. The next section describes how reconnection rates can be deduced from these observations.

3. Determining dayside and nightside reconnection rates

Changes in the open flux content of the magnetosphere are related to the rates of sub-solar magnetopause and magnetotail reconnection through Faraday's Law:

$$\frac{dF_{PC}}{dt} = \Phi_D - \Phi_N \tag{2}$$

where Φ_D and Φ_N are the rates (voltages) of creation and destruction of open flux at the low latitude dayside magnetopause and in the magnetotail, respectively (e.g. Siscoe and Huang, 1985). Another means of determining the dayside reconnection rate is to integrate the Y component of the motional electric field of the solar wind along an effective X-line length L_D, that is

$$\Phi_D = L_D V_{SW} B_S \,. \tag{3}$$

Here V_{SW} is the solar wind speed (effectively the plasma and magnetic flux inflow speed) and B_S is the southward component of the IMF defined as

$$B_S = \begin{cases} -B_z, & B_z < 0 \\ 0, & B_z > 0 \end{cases} \tag{4}$$

(we can similarly define the northward component B_N), which sets the sub-solar reconnection rate to zero when the IMF is directed northwards. Combining Eqs. 2 and 3

allows determination of the effective length of the reconnection X-line from the growth rate of the polar cap area (during periods when it can be assumed that $\Phi_N = 0$), and as demonstrated by Milan (2004a, b) and Milan *et al.* (2004, 2005b) this gives values of L_D in the range 5—8 R_E. This represents approximately 20% of the cross-wind scale size of the magnetosphere, and tallies nicely with the 20% reconnection efficiency determined by previous workers (e.g. Reiff *et al.*, 1981; Holzer *et al.*, 1986). We superimpose the growth of the polar cap estimated from Eqs. 2 and 3 for values of L_D = 5, 8, and 6 R_E, respectively, as dotted curves in panels a, f, and, k of Fig. 1; also shown are the corresponding times series of IMF B_z (panels c, h, and m) and Φ_D (panels d, i, and n). In each case, the observed rate of growth of F_{PC} is reproduced well by the prediction; although the value of L_D varies from interval to interval, within each interval L_D remains consistent. Understanding the variation of L_D between events requires further study.

Decreases in F_{PC} are caused by episodes of nightside reconnection, $\Phi_N > 0$. The occurrence, rate, and duration of these episodes can be found by fitting the model prediction to the data. We find that if it is assumed that the reconnection rate occurs at a uniform rate for a set length of time in each case, then a good fit can be achieved. Ten such episodes are identified during the three intervals shown in Fig. 1, with the variation of Φ_N being indicated in panels d, i, and n by grey rectangles, with the fitted model variation in F_{PC} being shown by the solid curves in panels a, f, and k. Bursts of reconnection last between 30 and 200 mins, at rates spanning 20 to 200 kV; in Section 4 we will look in more depth at these reconnection characteristics.

The onset of each nightside reconnection burst, indicated by vertical dashed lines, is not determined solely from the variation in F_{PC}, however. In most cases, significant substorm indicators are observed simultaneously, including Pi2 pulsations and the onset of associated magnetogram substorm bays. Also, break-up aurora are associated with substorms (marked SB) and lesser auroral brightenings (marked AB), which can be monitored by finding the maximum auroral luminosity observed on the nightside, I_{max}, shown in panels b, g, and l (equally, a spatially integrated auroral power could also be employed). The largest nightside reconnection bursts are associated with large enhancements in the auroral luminosity, smaller enhancements in brightness are associated with weaker reconnection bursts; indeed, a good correlation is found between I_{max} and Φ_N. In the main, the luminosity increases promptly at the onset of reconnection

(the discrepancy between onset and brightening at 10—11 UT, 26 August 1998, is due to only partial coverage of the nightside oval by the imager at this time), followed by a quasi-exponential decay to the background luminosity, though with occasional re-brightenings. The duration of the brightening and the reconnection burst are well correlated. The observations suggest that while the brightness decays gradually, the reconnection continues uniformly. We suggest that the initial increase in luminosity is associated with the formation of a near-Earth neutral line, and that the decay in luminosity represents the tailward motion of the X-line towards the distant neutral line.

The dayside and nightside reconnection rates are also related to the rate of transport of flux and plasma across the polar cap, quantified by the cross polar cap potential Φ_{PC}. There are two methods of measuring Φ_{PC}: (a) determine the voltage drop along a dawn-dusk cut of the polar cap, for instance with a polar orbiting spacecraft; (b) fully determine the electrostatic potential pattern associated with the convection (e.g. using the SuperDARN or AMIE techniques) and define Φ_{PC} as the difference between the maximum and minimum of the potential. In the former case, it can be shown that the cross polar cap potential will tend towards

$$\Phi_{PC} = \tfrac{1}{2}\left(\Phi_D + \Phi_N\right) + \Phi_V \tag{5}$$

(Lockwood and Cowley, 1992), where Φ_V is the voltage associated with any viscous-like interaction between the solar wind and the magnetopause, whereas the second method will give values closer to

$$\Phi_{PC} = \begin{cases} \Phi_D + \Phi_V, & \Phi_D > \Phi_N \\ \Phi_N + \Phi_V, & \Phi_D < \Phi_N \end{cases}. \tag{6}$$

As noted by Milan (2004b), care must be taken in comparing studies that have used different techniques for measuring the cross polar cap potential as Eq. 6 will consistently give greater estimates of Φ_{PC} than Eq. 5. Panels e, j, and o show Φ_{PC} calculated from Eq. 5, assuming $\Phi_V = 0$. The transpolar voltage remains non-zero for the majority of the intervals, even during periods when IMF $B_z > 0$ nT and dayside coupling is not expected; at these times, nightside reconnection drives the convection. These observations suggest that no viscous-like interaction need be invoked to explain the average residual cross polar cap potential during periods of IMF $B_z > 0$ nT (Milan, 2004b).

The discussion so far has concentrated on sub-solar and magnetotail reconnection, which cause the overall quantity of open flux in the magnetosphere to change. When IMF $B_z > 0$ nT, reconnection is expected to occur at high latitudes between the IMF and lobe field lines. This does not change the flux in the system, but rather stirs that which is already present. In this case, the rate of reconnection cannot be determined from observations of the polar cap size. However, as demonstrated by Milan *et al.* (2005b), the presence of transpolar arcs within the polar cap allow the movement of flux within the polar cap to be quantified. Such observations suggest that if the lobe reconnection rate is predicted from IMF observations in a similar manner to Eq. 3, substituting B_N for B_S, then the lobe reconnection X-line length deduced is of the order of 1 R_E. This predicts lobe reconnection rates that are consistent with those found by Chisham *et al.* (2004) from measurements of the associated ionospheric convection flow. Further work is needed to fully quantify the lobe reconnection rate, as we might expect it to depend on season and the IMF B_x component, both of which are known to modulate the reconnection geometries available at high latitudes.

4. Nightside reconnection rate and duration

In the intervals studied so far (including the three shown in Fig. 1), we have identified 14 nightside reconnection bursts. Of these, 9 display classical substorm signatures (SB) and 3 we classify as auroral brightenings (AB). Of the substorms, one is triggered by an external pressure pulse in the solar wind (see Milan *et al.*, 2004). The final event (NS – non-substorm) is a reconnection burst which occurs during northwards IMF, without substorm indicators, and with a characteristic convection signature previously described by Grocott *et al.* (2003, 2004, 2005) and Milan *et al.* (2005b). In this section we describe the characteristics of these events. Figure 2 presents histograms of (a) the polar cap flux prior to the onset of each event, (b) the flux remaining after each event, (c) the reconnection rate, (d) the event duration, and (e) the total flux closed during each burst. The latter is not necessarily equal to the difference between the flux before and after the event, as flux can be opened on the dayside during the course of the nightside burst. One event continued beyond the end of the measurement interval, so although the initial flux and reconnection rate could be calculated, the final flux, the event duration, and the flux closed are not known. As a

consequence, 14 events are shown in panels a and c; only 13 events are seen in panels b, d, and e.

In all cases the polar cap contained at least 0.5 GWb of open flux prior to onset, the average flux being nearly 0.8 GWb (Fig. 2a). The polar cap contracted to under 0.5 GWb during 9 out of 13 events (Fig. 2b). In the remaining events, on average 0.8 GWb of flux remained after the reconnection ceased; of these, two were auroral brightenings which did not close much flux, and of the remaining two substorms, the rate of dayside opening of flux was very high during one. We conclude that substorms tend to occur when 10% of the Earth's magnetic flux is open and in general continue until half of this flux has been closed.

The rate of reconnection (Fig. 2c) takes a wide variety of values between 30 and 200 kV, with no clear dependence on the classification of event. There is evidence (not shown) that the rate of reconnection is determined by the amount of open flux in the polar cap at the start of the event (excluding the externally triggered substorm): if $F_{PC} <$ 0.75 GWb, $\langle \Phi_N \rangle \approx 50$ kV, if $F_{PC} > 0.75$ GWb, $\langle \Phi_N \rangle \approx 100$ kV. As with the rate, the duration of the events (Fig. 2d) varies greatly, between 20 and 200 mins. The very longest events (over 100 mins) were all substorms. Finally, the total flux closed during each event (Fig. 2e) varied between just under 0.1 and 0.8 GWb. All auroral brightenings closed less than 0.3 GWb; all events that closed more than 0.4 GWb were substorms; on average, substorms closed 0.5 GWb of flux.

It is hoped that further investigation of reconnection rate and duration, polar cap flux, and external factors such as solar wind dynamic pressure at reconnection onset, might lead to a more comprehensive and quantitative understanding of substorm triggers.

5. Conclusions

Measurements of the flux content of the polar cap, using global auroral imagery, particle precipitation characteristics, and radar observations, allows the coupling between the solar wind, magnetosphere, and ionosphere, to be investigated. We find that the polar cap expands when the IMF is directed southwards and sub-solar reconnection creates new open flux. The polar cap contracts during episodes of magnetotail reconnection, usually associated with substorm onset. The reconnection starts promptly as the nightside auroral intensity increases at substorm onset; the

intensity thereafter decreases gradually, though the reconnection continues at a uniform rate, until the quiescent auroral state is re-attained. Reconnection events can last between 20 and 200 mins, at rates between 30 and 200 kV. The rate is perhaps related to the size of the polar cap at reconnection onset: the rate appears faster if the polar cap is larger and the tail is more stressed. In the events observed so far, reconnection only starts once the polar cap contains more than 0.5 GWb. The polar cap has not been observed to contain more than 1 GWb of flux, i.e. tail reconnection is usually initiated before this upper limit is reached.

The deduced dayside reconnection rates imply that reconnection is occurring across 20% of the width of the magnetosphere at any one time. On the other hand, observations of flux transfer events at the dayside magnetopause and their signatures in the ionosphere suggest that dayside reconnection occurs in quasi-episodic bursts which may last for 2 min, with a canonical repetition rate of 8 min (e.g. Lockwood and Smith, 1992). These two pieces of information, taken together, indicate that reconnection must occur in an on-off fashion across a very significant fraction of the dayside magnetopause. This may explain why transient reconnection signatures can be seen in the ionosphere in regions that map to the magnetospheric flanks (e.g. Milan *et al.*, 2000).

The measurements outlined in this paper not only allow the reconnection rates to be determined, but can also be employed to deduce the size and shape of the magnetotail, which is formed from those field lines which map to the polar cap (Dungey, 1961, 1965). Milan *et al.* (2004) showed that the tail inflates and deflates as the polar cap expands and contracts. In addition, knowing the size of the polar cap and the past rates of dayside and nightside reconnection, allow the length and flux content of the distant magnetotail to be deduced (Milan, 2004a). Such observations are a powerful tool for the diagnosis of the state of the terrestrial magnetosphere. Further work is necessary to quantify the change in polar cap flux for more events. This will allow investigation of the factors that control the length the dayside merging gap, and a more comprehensive statistical study of tail reconnection characteristics, including substorm triggering, reconnection rate and duration.

Finally, these ideas have recently been applied to other magnetospheres, esp. that of Saturn (Jackman *et al.*, 2004; Cowley *et al.*, 2005; Milan *et al.*, 2005a; Badman *et al.*, 2005). It is hoped that in this way we will gain a generalized insight into the physics of

solar wind-magnetosphere coupling that applies to all magnetized solar system bodies, not just Earth.

References

Badman, S. V., E. J. Bunce, J. T. Clarke, S. W. H. Cowley, J.-C. Gérard, D. Grodent, and S. E. Milan, Open flux estimates in Saturn's magnetosphere during the January 2004 Cassini-HST campaign, and implications for reconnection rates, *J. Geophys. Res.*, submitted, 2005.

Baker, K. B., A. S. Rodger, and G. Lu, HF-radar observations of the dayside magnetic merging rate: A Geospace Environment Modeling boundary layer campaign study, *J. Geophys. Res.*, *102*, 9603-9617, 1997.

Blanchard, G. T., C. L. Ellington, L. R. Lyons, and F. J. Rich, Incoherent scatter radar identification of the dayside magnetic separatrix and measurement of magnetic reconnection, *J. Geophys. Res.*, *106*, 8185-8195, 2001.

Chisham, G., and M. P. Freeman, A technique for accurately determining the cusp-region polar cap boundary using SuperDARN HF radar measurements, *Ann. Geophysicae*, *21*, 983-996, 2003.

Chisham, G., M. P. Freeman, I. J. Coleman, M. Pinnock, M. R. Hairston, M. Lester, and G. Sofko, Measuring the dayside reconnection rate during an interval of due northward interplanetary magnetic field, *Ann. Geophysicae*, *22*, 4243-4258, 2004.

Chisham, G., M. P. Freeman, T. Sotirelis, R. A. Greenwald, M. Lester, J.-P. Villain, A statistical comparison of SuperDARN spectral width boundaries and DMSP particle precipitation boundaries in the morning sector ionosphere, *Ann. Geophysicae*, *23*, 733-743, 2005.

Cowley, S. W. H., Magnetospheric and ionospheric flow and the interplanetary magnetic field, in *The Physical Basis of the Ionosphere in the Solar-Terrestrial System*, AGARD CP-295, 4(1)-4(14), 1981.

Cowley, S. W. H., S. V. Badman, E. J. Bunce, J. T. Clarke, J.-C. Gérard, D. Grodent, C. M. Jackman, S. E. Milan, and T. K. Yeoman, Reconnection in a rotation-dominated magnetosphere and its relation to Saturn's auroral dynamics, *J. Geophys. Res.*, *110*, A02201, doi: 10.1029/2004JA010796, 2005.

Cowley, S. W. H., and M. Lockwood, Excitation and decay of solar wind-driven flows in the magnetosphere-ionosphere system, *Ann. Geophysicae*, *10*, 103-115, 1992.

de la Beaujardiere, O., L. R. Lyons, and E. Friis-Christensen, Sondrestrom radar measurements of the reconnection electric field, *J. Geophys. Res.*, *96*, 13907-13912, 1991.

Dungey, J. W., Interplanetary magnetic fields and the auroral zones, *Phys. Rev. Letters*, 6, 47-48, 1961.

Dungey, J. W., The structure of the exosphere or adventures in velocity space, in *Geophysics, The Earth's Environment*, eds. C. De Witt, J. Hieblot, and L. Le Beau, Gordon and Breach, New York, p. 503-550, 1963.

Dungey, J. W., The length of the magnetospheric tail, *J. Geophys. Res.*, 70, 1753, 1965.

Frank, L. A., and J. D. Craven, Imaging results from Dynamics Explorer 1, *Rev. Geophys.*, *26*, 249-283, 1988.

Grocott, A., S. V. Badman, S. W. H. Cowley, T. K. Yeoman, and P. J. Cripps, The influence of IMF B_y on the nature of the nightside high-latitude ionospheric flow during intervals of positive IMF B_z, *Ann. Geophysicae*, 22, 1755-1764, 2004.

Grocott, A., S. W. H. Cowley, and J. B. Sigwarth, Ionospheric flow during extended intervals of northward but B_y-dominated IMF, *Ann. Geophysicae*, 21, 509-538, 2003.

Grocott, A., S. W. H. Cowley, J. B. Sigwarth, J. F. Watermann, and T. K. Yeoman, Excitation of twin-vortex flow in the nightside high latitude ionosphere during an isolated substorm, *Ann. Geophysicae*, 20, 1577-1601, 2002.

Grocott, A., T. K. Yeoman, S. E. Milan, and S. W. H. Cowley, Interhemispheric observations of the ionospheric signature of tail reconnection during IMF-northward non-substorm intervals, *Ann. Geophysicae*, *23*, 1763-1770, 2005.

Holzer, R. E., R. L. McPherron, and D. A. Hardy, A quantitative empirical model of the magnetospheric flux transfer process, *J. Geophys. Res.*, 91, 3287-3293, 1986.

Jackman, C. M., N. Achilleos, E. J. Bunce, S. W. H. Cowley, M. K. Dougherty, G. H. Jones, S. E. Milan, and E. J. Smith, Interplanetary magnetic field at ~9 AU during the declining phase of the solar cycle and its implications for Saturn's magnetospheric dynamics, *J. Geophys. Res.*, *109*, A11203, doi: 10.1029/2004JA010614, 2004.

Lockwood, M., and S. W. H. Cowley, Ionospheric convection and the substorm cycle, in *Proceedings of the International Conference on Substorms (ICS-1)*, 99-109, 1992.

Lockwood, M., and M. F. Smith, The variation of reconnection rate at the dayside magnetopause and cusp ion precipitation, *J. Geophys. Res.*, 97, 14841-14847, 1992.

Milan, S. E., A simple model of the flux content of the distant magnetotail, *J. Geophys. Res.*, 109, A07210, doi: 10.1029/2004JA010397, 2004a.

Milan, S. E., Dayside and nightside contributions to the cross polar cap potential: placing an upper limit on a viscous-like interaction, *Ann. Geophysicae*, *22*, 3771-3777, 2004b.

Milan, S. E., E. J. Bunce, S. W. H. Cowley, and C. M. Jackman, Implications of rapid planetary rotation for the Dungey magnetotail of Saturn, *J. Geophys. Res.*, *110*, A03209, doi: 10.1029/2004JA010716, 2005a.

Milan, S. E., S. W. H. Cowley, M. Lester, D. M. Wright, J. A. Slavin, M. Fillingim, C. W. Carlson and H. J. Singer, Response of the magnetotail to changes in open flux content of the magnetosphere, *J. Geophys. Res.*, *109*, A04220, doi: 10.1029/2003JA010350, 2004.

Milan, S. E., B. Hubert, A. Grocott, and F. Creutzberg, Formation and motion of a transpolar arc in response to dayside and nightside reconnection, *J. Geophys. Res.*, *110*, A01212, doi: 10.1029/2004JA010835, 2005b.

Milan, S. E., M. Lester, S. W. H. Cowley, and M. Brittnacher, Dayside convection and auroral morphology during an interval of northward interplanetary magnetic field, *Ann. Geophysicae*, *18*, 436-444, 2000.

Milan, S. E., M. Lester, S. W. H. Cowley, K. Oksavik, M. Brittnacher, R. A. Greenwald, G. Sofko, and J.-P. Villain, Variations in polar cap area during two substorm cycles, *Ann. Geophysicae*, *21*, 1121-1140, 2003.

Mishin, V. M., L. P. Block, A. D. Bazarzhapov, T. I. Saifudinova, S. B. Lunyushkin, D. Sh. Shirapov, J. Woch, L. Eliasson, G. T. Marklund, L. G. Blomberg, and H. Opgenoorth, A study of the CDAW 9C substorm of May 3, 1986, using magnetogram inversion technique 2, and a substorm scenario with two active phases, *J. Geophys. Res.*, 102, 19845-19859, 1997.

Pinnock, M., and A. S. Rodger, On determining the noon polar cap boundary from SuperDARN HF radar backscatter characteristics, *Ann. Geophysicae*, *18*, 1523-1530, 2001.

Reiff, P. H., and J. L. Burch, IMF B_y-dependent plasma flow and Birkeland currents in the dayside magnetosphere, 2. A global model for northward and southward IMF, *J. Geophys. Res.*, *90*, 1595-1609, 1985.

Reiff, P. H., R. W. Spiro, and T. W. Hill, Dependence of polar cap potential drop on interplanetary parameters, *J. Geophys. Res.*, 86, 7639-7648, 1981.

Russell, C. T., The configuration of the magnetosphere, in *Critical Problems of Magnetospheric Physics*, ed. E. R. Dyer, Inter-Union Committee on Solar Terrestrial Physics, National Academy of Sciences, Washington, D.C., p. 1-16, 1972.

Sotirelis, T., P. T. Newell, C.-I. Meng, Shape of the open-closed boundary of the polar cap as determined from observations of precipitating particles by up to four DMSP satellites, *J. Geophys. Res.*, *103*, 399-406, 1998.

Siscoe, G. L., and T. S. Huang, Polar cap inflation and deflation, *J. Geophys. Res.*, 90, 543-547, 1985.

Taylor, J. R., T. K. Yeoman, M. Lester, B. A. Emery, and D. J. Knipp, Variations in the polar cap area during intervals of substorm activity on 20-21 March 1990 deduced from AMIE convection maps, *Ann. Geophysicae*, *14*, 879-887, 1996.

Wild, J. A., S. E. Milan, C. J. Owen, J. M. Bosqued, M. Lester, D. M. Wright, H. Frey, C. W. Carlson, A. N. Fazakerley, and H. Rème, On the determination of the open-closed magnetic field line boundary location in the dusk sector auroral ionosphere: global auroral imaging, coherent scatter radar and energetic particle observations, *Ann. Geophysicae*, *22*, 3625-3639, 2004.

Figures

Figure 1. Measurements related to the investigation of dayside and nightside reconnection for three events on 5 June 1998 (panels a—e), 26 August 1998 (panels f—j), and 19 January 2002 (panels k—o). Vertical dashed lines (labelled in panels c, h, m) indicate the onsets of substorms and auroral brightenings. (Panels a, f, k) Observed variation in polar cap flux (grey), predicted polar cap flux, including and excluding the contribution from nightside reconnection (solid and dotted, respectively). (Panels b, g, l) Maximum auroral intensity on the nightside, I_{max}. (Panels c, h, m) IMF B_z lagged to the magnetopause. (Panels d, i, n) Deduced day- and nightside reconnection rates, Φ_D and Φ_N. (Panels e, j, o) Cross polar cap potential calculated from Eq. 5.

Figure 2. Histograms of (a) polar cap flux at onset of tail reconnection, (b) flux remaining at end, (c) nightside reconnection rate, (d) reconnection duration, and (e) overall flux closed. Events are categorized by type (see text).

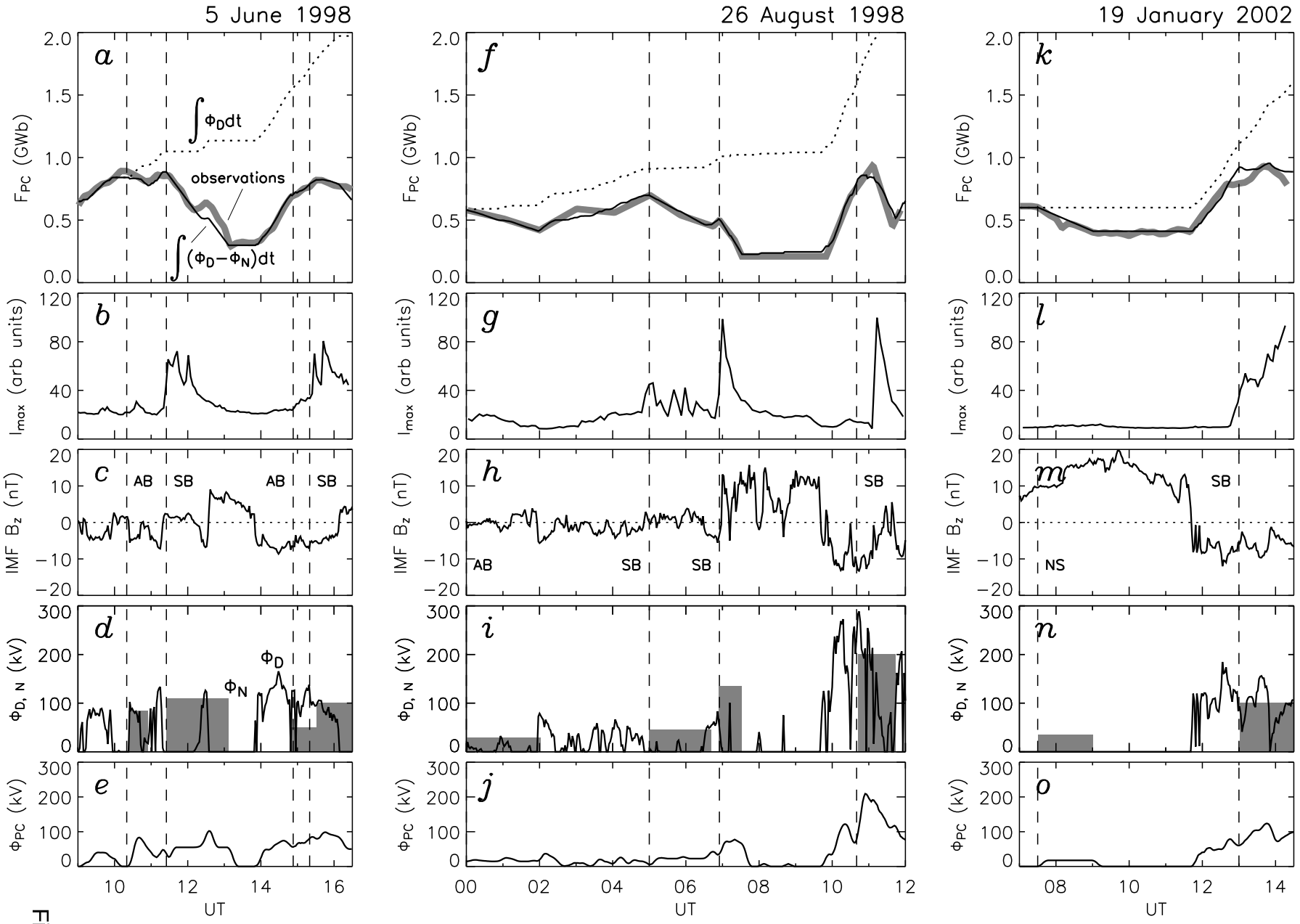
5 June 1998
26 August 1998
19 January 2002
a
b
c
d
e
f
g
h
i
j
k
l
m
n
o
F_{PC} (GWb)
$\int \Phi_D dt$
observations
$\int (\Phi_D - \Phi_N) dt$
I_{max} (arb units)
IMF B_z (nT)
AB
SB
NS
$\Phi_{D,N}$ (kV)
Φ_D
Φ_N
Φ_{PC} (kV)
UT

Figure 1

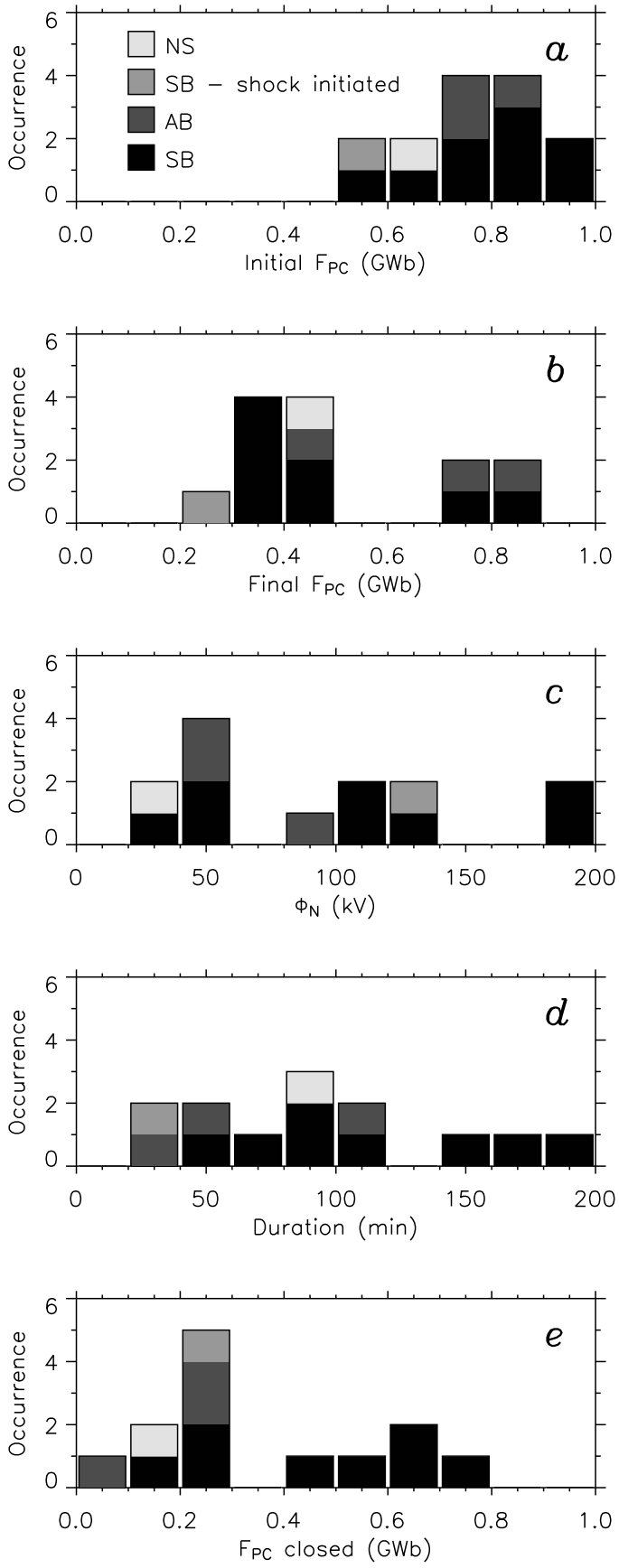
a
NS
SB – shock initiated
AB
SB
Occurrence
Initial F_{PC} (GWb)
b
Occurrence
Final F_{PC} (GWb)
c
Occurrence
Φ_N (kV)
d
Occurrence
Duration (min)
e
Occurrence
F_{PC} closed (GWb)

Figure 2